ACS Chemical Neuroscience

Letter

pubs.acs.org/chemneuro

# Visualization of Lipid Raft Membrane Compartmentalization in Living RN46A Neuronal Cells Using Single Quantum Dot Tracking

Jerry C. Chang[†] and Sandra J. Rosenthal*[,†,‡,§]

[†]Department of Chemistry and [‡]Departments of Pharmacology, Chemical and Biomolecular Engineering, Physics and Astronomy, and Vanderbilt Institute of Nanoscale Science and Engineering, Vanderbilt University, Nashville, Tennessee, United States

[§]Materials Science and Technology Division, Oak Ridge National Laboratory, Oak Ridge, Tennessee, United States

Supporting Information

**ABSTRACT:** Lipid rafts are cholesterol-enriched subdomains in the plasma membrane that have been reported to act as a platform to facilitate neuronal signaling; however, they are suspected to have a very short lifetime, up to only a few seconds, which calls into question their roles in biological signaling. To better understand their diffusion dynamics and membrane compartmentalization, we labeled lipid raft constituent ganglioside GM1 with single quantum dots through the connection of cholera toxin B subunit, a protein that binds specifically to GM1. Diffusion measurements revealed that single quantum dot-labeled GM1 ganglioside complexes undergo slow, confined lateral diffusion with a diffusion coefficient of ~7.87 × $10^{-2}$ $\mu m^2/s$ and a confinement domain about 200 nm in size. Further analysis of their trajectories showed lateral confinement persisting on the order of tens of seconds, comparable to the time scales of the majority of cellular signaling and biological reactions. Hence, our results provide further evidence in support of the putative function of lipid rafts as signaling platforms.

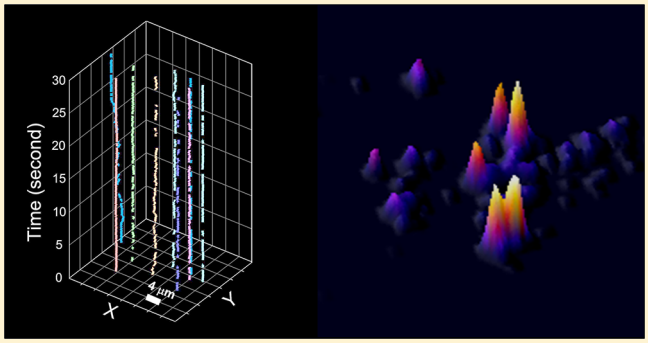


**KEYWORDS:** *Quantum dot, single-molecule imaging, lipid rafts, membrane dynamics, trafficking*

Cholesterol-enriched membrane microdomains, known as lipid rafts, have been proposed to participate in cellular signal transduction by providing the microenvironment necessary for complex protein−protein interactions.[1−3] Early evidence based on simplified membrane models showed that the presence of rigid cholesterol in the membrane essentially acts as glue, which packs the sphingolipids and unsaturated phospholipids closely together to form a highly directional, organized, and detergent-resistant state.[1] These specialized membrane domains were found abundantly in neuronal cells and contained sets of associated proteins, especially the glycosyl-phosphatidylinositol (GPI)-anchored proteins, and were hypothesized to facilitate the regulation of membrane proteins through establishing boundaries between the rafts and fluid compartments in the plasma membrane.[1,2] The roles of lipid rafts in neuronal signaling have received increased attention in recent years.[4] However, studies on how lipid rafts participate in neuronal signaling still mostly rely on biochemical methods, such as using detergents to isolate the insoluble membrane fraction,[5] which lack dynamic information to help decipher the roles of lipid rafts in membrane compartmentalization.

Single-molecule imaging is well-known for revealing dynamic information in living cells.[6−8] Real-time tracking of single-molecules in living cells are typically accomplished with the use of fluorescent dye labels or polymeric particles.[6] Most of the difficulties in implementing single-molecule imaging arise from the characteristics of these traditional probes, in particular their poor photostability or exceedingly large size compared with the targeted molecule.[6] Recently, fluorescent quantum dots (QDots), which surpass the above limitations, have found widespread applications in biological sciences.[9,10] Specifically, real-time tracking based on a single QDot approach has emerged as a powerful tool for probing membrane protein dynamics in living cells.[10] In 2003, Dahan and co-workers reported single QDot tracking of individual glycine receptors in living neurons.[11] This pioneering study made it possible to reveal multiple diffusion domains of glycine receptors in synaptic, perisynaptic, and extrasynaptic locations. Similar approaches were then employed for the studies of various targets in neuronal signaling, including the nerve growth factor,[12] the γ-aminobutyric acid A receptor ($GABA_AR$),[13] and more recently, the serotonin transporter.[14]

In this paper, we adopt the single QDot tracking method to investigate the membrane dynamics of lipid raft constituent ganglioside GM1 in living RN46A neuronal cells. Using high-speed, line-scanning confocal microscopy, we demonstrated that our QDot-based imaging paradigm is sufficient to provide a spatial resolution down to the single-molecule level. Importantly, our data point to long-term stability of lipid rafts, as

**Published:** August 1, 2012

   dx.doi.org/10.1021/cn3000845 | ACS Chem. Neurosci. 2012, 3, 737−743

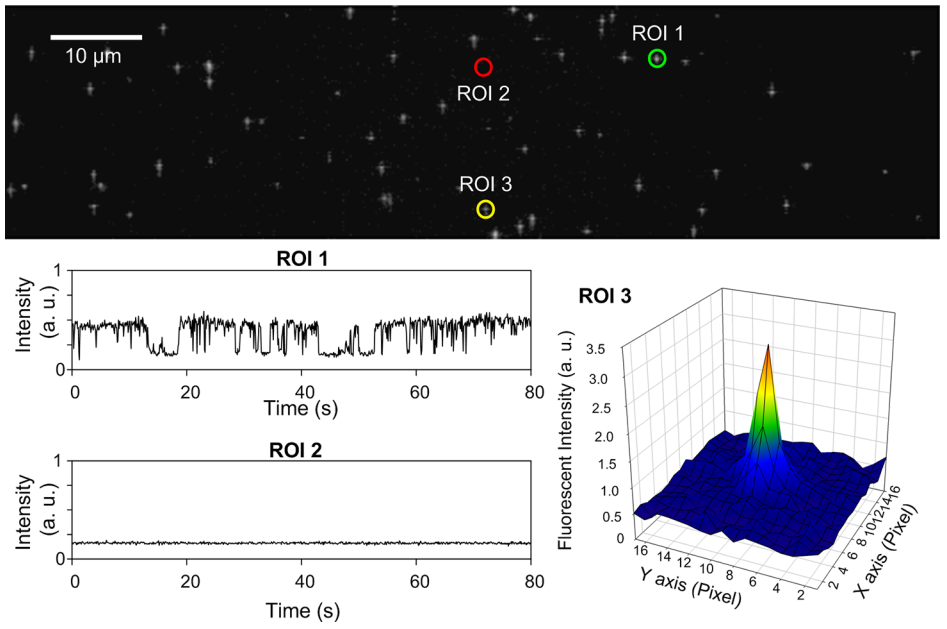


**Figure 1.** Visualization of single QDots on a glass support. Upper panel provides a single frame from time lapse imaging of QDots taken with the high-speed line scanning confocal microscope at 10 Hz scan rate. Spin-casting ITK carboxyl-modified 605 nm QDots were immobilized on the glass coverslip bottomed MetTek dish for imaging. Two randomly selected blinking QDots (ROI 1, ROI 3) and a randomly selected background region (ROI 2) are indicated by circles. Scale bar =10 $\mu$m. Lower left panels provide time-dependent intensity traces of the selected ROIs. Fluorescence intensity of ROI 1 QDot is constant during the "on" state and shifts to a similar intensity level as background indicated by the intensity time trace of ROI 2. A 3D intensity plot of QDot (ROI 3) was used to provide an estimate of the spatial resolution achieved with our imaging paradigm (central position uncertainty = ± 10−15 nm, one pixel =200 nm).

single QDot-labeled GM1 complexes show lateral confinement persisting on the order of tens of seconds.

## RESULTS AND DISCUSSION

To determine the spatial and temporal resolution of our imaging approach, carboxyl functionalized, amphiphilic poly(acrylic acid) polymer-coated QDots (AMP QDots) were first spin-cast onto a cover glass and then observed on a line-scanning confocal microscope system (Figure S1, Supporting Information).[15] Time-lapse fluorescence imaging of QDots was used to assess temporal and spatial characteristics of single QDot fluorescence (Figure 1, upper panel). In addition, we demonstrated a pattern of fluorescence intermittency ("blinking"), a criterion for single QDot detection (Figure 1, lower left panel).[16,17] Furthermore, the intensity distribution coming from a single QDot shows a diffraction-limited pattern (Figure 1 ROI 3, lower right panel), representing an important signature of single molecules.[18] Further analysis using 2D Gaussian fit of the intensity distribution provides an estimate of the localization of a single QDot with accuracy measured at ∼10−15 nm (see Methods).[19]

Previous works from our laboratory have indicated that water-soluble AMP QDots, which were generated from passivating the hydrophobic QDots with amphiphilic polymers, nonspecifically interact with the cellular membrane via hydrophobic interaction.[20,21] This artifact of QDot biological labeling to the plasma membrane turns out to be a successful molecular probe as a background staining for studying the mobility of the neuronal membrane. To ensure the spatial separation of single QDots in regions greater than the diffraction-limited distance for single-molecule tracking, AMP QDots are used at an extremely low concentration (<10 pmol) in RN46A cells. Figure 2A shows typical trajectories of AMP QDots on the surface of a living RN46A cells. Although various moving patterns can be observed, the majority of trajectories exhibit a distinct, Brownian-type motion mode. We must also note that neither distinct orientation nor clear membrane compartmentalization (i.e., restricted movement in trajectories) is predominantly displayed (Figure S2, Supporting Information), suggesting that no particular force governs the motion of AMP QDots in the plasma membrane. To gain a quantitative assessment of the velocity of the diffusing QDots, we analyzed the distribution of instantaneous velocity (single step displacement over a time increment, $\tau$ = 100 ms, see Methods). As shown in Figure 2B, single AMP QDots nonspecifically bound to the membrane display a bimodal distribution of instantaneous velocity with a majority falling in the fast population ($\nu_{slow}$ = 0.51 ± 0.03 $\mu$m/s, 11.6%; $\nu_{fast}$ =1.46 ± 0.04 $\mu$m/s, 88.4%).

To perform single QDot tracking of the lipid raft constituent ganglioside GM1, a two-step labeling approach was implemented in which RN46A cells were initially incubated with biotinylated cholera toxin B subunit (CTxB),[22,23] a protein that binds specifically to ganglioside GM1, followed by the incubation with streptavidin-conjugated QDots (SA-QDots) (see Methods). Labeling of only single QDot conjugates was further evaluated via blinking behavior inspection (Figure 3A). Shown in Figure 3B are typical trajectories of single QDot−GM1 complexes in the membrane of RN46A cells, where apparently only confined motion can be found. The analysis of the distribution of instantaneous velocity was then carried out to correlate the confined movements (Figure 3C). As expected, the distribution fits a single population well and the fitted instantaneous velocity was estimated as $\nu$ = 0.88 ± 0.03 $\mu$m/s (see Methods).

The dependence of the mean square displacement (MSD) on the time interval, which provides an estimate for the


dx.doi.org/10.1021/cn3000845 | ACS Chem. Neurosci. 2012, 3, 737−743

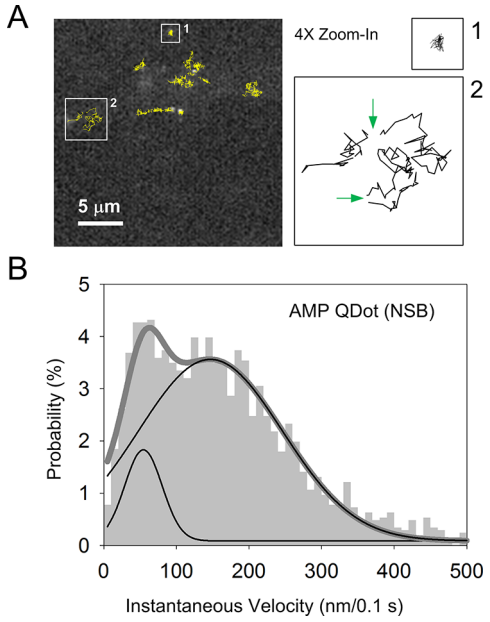


**Figure 2.** Trajectories and instantaneous velocity of AMP QDots nonspecifically bound to the plasma membrane of living RN46A cells. (A) A single frame from a time-lapse recording of single AMP QDots diffusing in the native membrane of a RN46A cell that was superimposed upon the trajectories throughout the recording. Trajectories on the right are 4× zoom-in of the selected ones on the left, and green arrows note the blinking events. Although the motion of AMP QDots can be generally categorized as being one of two types, confined (as indicated in box 1) or nonconfined (as indicated in box 2); most trajectories show a nonconfined pattern. (B) The instantaneous velocity plot of AMP QDots is shown for the data from 4122 steps. The data points are well-fitted to a bimodal distribution where a majority falling in the fast population ($\nu_{slow}$ = 0.51 ± 0.03 μm/s, 11.6%; $\nu_{fast}$ =1.46 ± 0.04 μm/s, 88.4%).

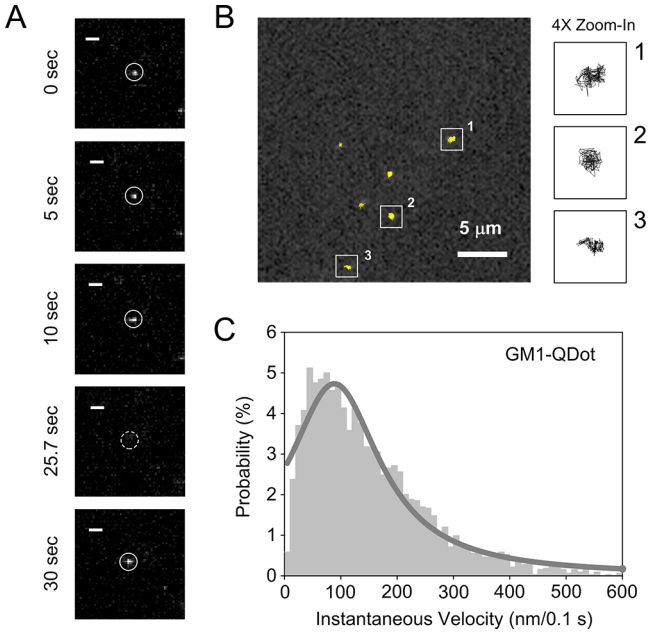


**Figure 3.** Trajectories and instantaneous velocity of single QDot-conjugated GM1 complexes in the plasma membrane of living RN46A cells. (A) Representative snapshots from a time-lapse series of single QDot−GM1 complexes via the bridge of CTxB. The white circles indicate the QDot being followed, and the dashed circle ($t$ = 25.7 s) notes a blinking event (scalebar = 1.5 μm). (B) A single frame from a time-lapse recording of single QDots bound to GM1 in the native membrane of a RN46A cell that was superimposed upon the trajectories throughout the recording. Three representative trajectories (right boxes) show a confined motion pattern and their 4× zoom-in (left boxes) are displayed. (B) The instantaneous velocity plot of AMP QDots is shown for the data from 3240 steps. The data points are well-fitted to a single distribution ($\nu$ = 0.88 ± 0.03 μm/s).

diffusion mode of a trajectory,[24,25] was then used to dissect the lateral diffusion and membrane confinements (Figure 4). As seen in Figure 4A, the diffusion of AMP QDots in the membrane appears to be Brownian since a linear correlation of MSD with time can be observed. From the linear fit, we obtained a diffusion coefficient $D$ = 0.393 ± 0.002 μm$^2$/s (mean ± SEM) similar to the reported diffusion coefficients of lipid probes in the native membrane on the order of 0.1−1 μm$^2$/s.[26] In comparison, the MSD versus time plot of single QDot-labeled ganglioside GM1 shows a curvature, indicating restricted diffusion. Consequently, a confined diffusion mode was used to calculate the diffusion coefficient and the characteristic size of the short-term confining domain $L$ (see Methods), yielding the values of $D$ = (7.87 ± 0.04) × 10$^{-2}$ μm$^2$/s and $L$ = 198 ± 33 nm. The diffusion distributions of AMP QDots and QDot-labeled GM1 were further evaluated using a cumulative probability plot (Figure 4C). Although visual inspection shows minimal overlap between the two cases, the diffusion coefficients of QDot-labeled GM1 are mostly restricted to the slow time scales (10$^{-2}$−10$^{-3}$ μm$^2$/s), whereas AMP QDots in the membrane diffuse significantly faster ($p$ value < 0.05, Shapiro−Wilk test) and exhibit a large range of diffusion rates.

The diffusion dynamics of QDot-labeled GM1 molecules in comparison to AMP Qdots suggests that lipid rafts in the cell membrane produce a strong stabilization effect. We therefore sought to take advantage of the inherent photostability of QDots to follow GM1 movements over longer time scales (seconds to tens of seconds). Shown in Figure 5 is a spatiotemporal 3D graph of single QDot-labeled GM1 complexes in the native membrane of RN46A cells, where the majority of individual QDot−GM1 complexes exhibit movements less than 1 μm in distance throughout the entire recording. In comparison, ∼80% of the AMP QDots display overall movement larger than 1 μm (Figure S2B, Supporting Information, $n$ = 43).

The diffusion coefficient, $D$, dwelling time, $\tau$, and putative confinement domain, $L$, of lipid rafts have been previously estimated by various approaches. The study presented herein was designed to directly follow the motion of a lipid raft constituent GM1, while the native membrane integrity was preserved. Using a single QDot labeling approach, we reveal that GM1 comprised lipid rafts slowly diffuse within a confinement zone, which has a diameter of ∼200 nm. Further inspection of the long-term time-dependent trajectories (Figure 5) features the persistent confinement of lipid rafts in RN46A cells ($L$ = 200 nm, $D$ = 7.8 × 10$^{-2}$ μm$^2$/s, $\tau$ > 10 s). In comparison, Schütz et al. adopted liposome-facilitated delivery of a saturated acyl-chain fluorescent lipid probe (1,2-dimyristoyl-*sn*-glycero-3-phosphoethanolamine, DMPE-Cy5) for single-molecule tracking. In their analyses, lipid rafts were found to be localized in relatively larger partitioning domains along with faster diffusion rates and a long dwelling time in HSAM cells ($L$ = 0.2−2 μm, $D$ = 0.6−0.9 μm$^2$/s, $\tau \approx$ 13 s).[27] Interestingly, a recent stimulated emission depletion (STED)


dx.doi.org/10.1021/cn3000845 | ACS Chem. Neurosci. 2012, 3, 737−743

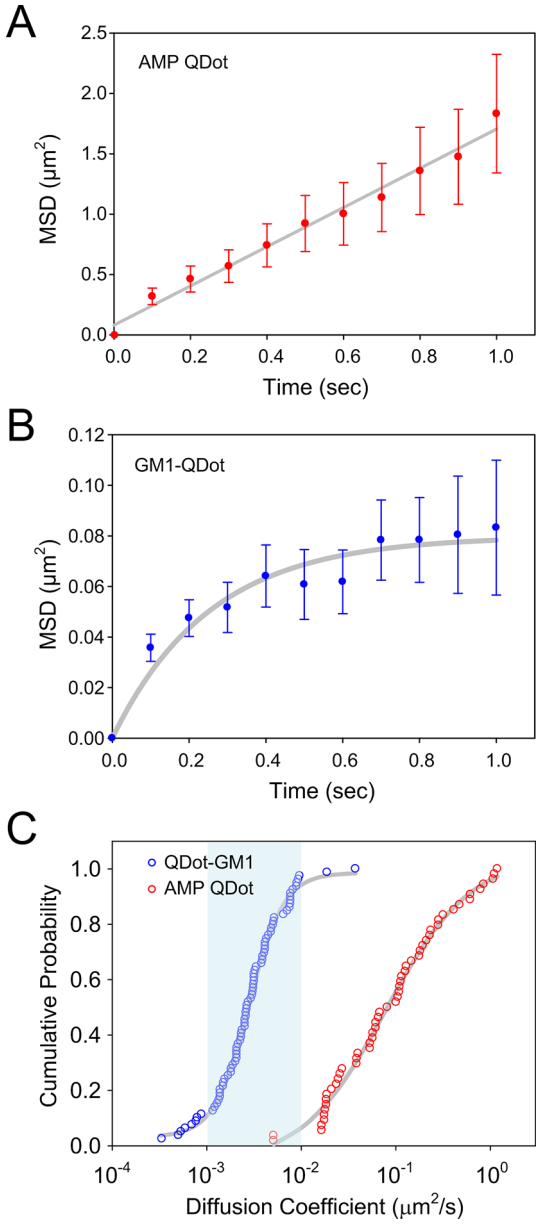


**Figure 4.** Comparison of diffusion behavior of single AMP QDots and QDot-labeled GM1 complexes in the RN46A cells. (A) Averaged MSD as a function of time for single AMP QDots. Solid gray line is computed based on linear regression, indicating a simple diffusion. (B) Averaged MSD as a function of time for single QDot−GM1 complexes. Solid gray curve is the best fit based on an exponential function (see Methods), indicating a confined diffusion. (C) Cumulative distribution of the diffusion coefficients. Blue shadow, which indicates $10^{-3} < D < 10^{-2}$, is used for visual comparison.

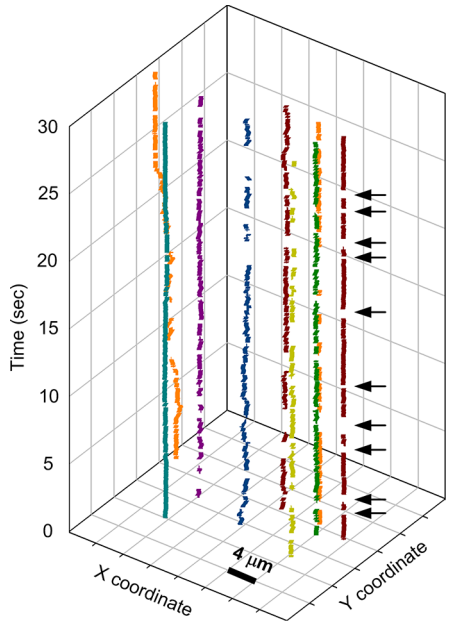


**Figure 5.** Spatiotemporal 3D representation of movement of the single QDot−GM1 complexes in living RN46A cells. Fluorescent intermittency ("blinking") of a single QDot on an example trajectory is noted by black arrows.

microscopy study reported by Eggeling et al. showed that lipid raft-associated constituents, including the sphingolipids and GPI-anchored proteins, are transiently trapped in nanoscale domains for only tens of milliseconds with a relatively slower diffusion rate in the PtK2 cells ($L$ < 20 nm, $D = 2 \times 10^{-2}$ $\mu m^2/s$, $\tau$ = 10−20 ms).[28] Because lipid rafts are known to contain various components and participate in dynamic membrane trafficking and signaling, it is perhaps not surprising that differences in detecting approaches, experimental time resolutions, targeted molecules, and cell models would have a substantial impact on the estimates of raft diffusion properties. Clearly, a systematic examination of various lipid raft constituents is required for a more general understanding of membrane dynamics of lipid rafts.

Presently how lipid rafts contribute to biological signaling is an open question. A closely related point of view is that for a lipid raft to be able to act as a signaling platform, the lifetime of a lipid raft should be at least partially relevant to a biological signaling duration (i.e., the time scales over which biological signaling persists). Since protein signaling networks typically operate on time scales of seconds to minutes, the lifetime of lipid rafts are likely to exist on similar time scales, which is consistent with the findings reported in this study. In addition, if lipid rafts are membrane subdomains that facilitate the signaling of raft-associated proteins, proteins residing in the lipid rafts should share a similar confined diffusion mode as we observed in this research. In a recent study, Andrews et al. followed the motion of individual high-affinity IgE receptors (FcεRI), a class of raft-dependent receptors, with monovalent antibody-conjugated QDots in living cells and identified confined diffusion with seconds of cross-linking in FcεRI signaling.[29] A similar confined diffusion mode was observed with single QDot labeled GPI anchored proteins,[30] α7 neuronal nicotinic acetylcholine receptors,[31] and serotonin transporters.[14] However, the question of whether lipid rafts dynamically govern protein signaling remains unanswered. Consequently, a multichannel single QDot tracking protocol for simultaneous multitarget analysis (i.e., one color of QDot labeling for raft constituent and another color of QDot labeling for the raft-associated protein) may hold high potential in the acquisition of information to address the above question.

As mentioned in the introduction, common attempts to perform real-time tracking of membrane constituents mostly rely on the use of organic fluorophores or micrometer to submicrometer-sized polymeric particles. The main advantage of organic fluorophores in real-time tracking is their small size (≤1 nm). This property makes them particularly useful for


dx.doi.org/10.1021/cn3000845 | ACS Chem. Neurosci. 2012, 3, 737−743

tracking movements of individual receptors in distinct subcellular structures such as synapse or caveolae.[32] Until now, the real bottleneck of dye-based single-molecule microscopy is still the photostability of the organic fluorophores, which limits the tracking time to only a few seconds.[6,32] In contrast, polymeric particles, owing to their superior strength in photostability, have been popularly used for following membrane dynamics since the 1990s.[25] However, the large size of the particles (>100 nm), which inevitably leads to cross-linking of the labeling targets, call into question the diffusion characteristics measured.[33] So how can we address these shortcomings from both sides? The current best compromise is perhaps the use of photostable QDots for real-time tracking. Although the diameter of QDots compared with the organic fluorophores is still relatively large (10−20 nm) and the monovalent QDots are not commercially accessible, with appropriate adjustment in conjugation protocol (i.e., fine-tune the QDot/ligand molar ratio in conjugation conditions)[26,34] single QDot tracking can be regarded as a single-molecule technique. Importantly, differences of QDot-conjugated and dye-conjugated approaches in measured diffusion coefficients are minimal,[11,26,32] indicating the applicability of QDots to substitute organic fluorophores for single-molecule tracking.

In conclusion, our single-QDot tracking study documents the diffusion properties of ganglioside GM1 in the plasma membrane of RN46A cells. The valuable information on membrane dynamics of lipid rafts as well as our straightforward, readily transferrable single QDot experimental protocol presented herein may form a basis for not just raft studies but also membrane protein research in living cells. It will be interesting to dissect the functional implications of the lateral confinement of lipid rafts in the neuronal membrane. In a preliminary treatment study, we observed a non-Brownian, actin cytoskeleton-dependent membrane dynamic in GM1 movements.[14] Further analysis of the connection between lipid rafts and cytoskeleton may yield useful insights into the compositional heterogeneity of lipid raft-associated signaling.[2]

## METHODS

**Single QDot Labeling of Ganglioside GM1 in RN46A Cells.** The immortalized serotonergic neural cell line, RN46A, was provided by Dr. Whittemore (University of Miami School of Medicine).[35] RN46A cells were cultured in DMEM/F12 (1:1; Life Technologies, Grand Island, NY) supplemented with 10% FBS and incubated in a humidified atmosphere with 5% $CO_2$ at 37 °C. For experiments involving the labeling of ganglioside GM1 in the plasma membrane, RN46A cells were first incubated with 200 nM biotinylated CTxB (CTxB/biotin molar ratio ~1:1 to avoid cross-linking, Sigma, St. Louis, MO) for 30 min prior to a 5 min 0.5 nM SAv-QDot (Life Technologies, Grand Island, NY) incubation. Importantly, ganglioside GM1−CTxB association has been shown to elicit endocytosis.[22] To avoid endocytosis and to achieve successful assessments in membrane dynamics, all optical live-cell time-lapse image series were taken immediately after QDot labeling.

**Microscopy.** Confocal images were obtained on a Zeiss LSM 5 Live confocal system (Carl Zeiss Jena GmbH, Jena, Germany) and viewed with a Zeiss 63×/1.4 NA oil immersion objective lens. Excitation was provided by a 488 nm 100-mW diode laser. Single QDot emission was collected using a bandpass 610/20 mm filter (for QDot 605) or a long pass 650 mm filter (for QDot 655). Each sequence of time-lapse images was acquired at 10 frames per second for 30−60 s with a scan format of 512 × 128 pixels. All live-cell imaging was performed at 37 °C. Analysis of raw data images was processed using Zeiss LSM image examiner.

**Subpixel Localization and Trajectory Generation.** To calculate a subpixel estimate of single QDot position, the single QDot intensity distribution (Figure 1C) was fitted with a 2D Gaussian function:[19] $I_{xy} = A_0 + A\, e^{-[(x-x_0)^2+(y-y_0)^2]/w^2}$, where $I_{xy}$ is the intensity of the pixel, $x_0$ and $y_0$ are the designated local maximum coordinates of the Gaussian, $A$ is the amplitude of the signal with local background, $A_0$, and $w$ is the width of the Gaussian curve. Note that the coordinate ($x_0$, $y_0$) acquired by 2D Gaussian fit is not a true position but only an estimate. The accuracy is dependent upon the respective signal-to-noise ratio (SNR), which is defined as SNR = $I_0/(\sigma_{bg}^2 + \sigma_{I_0}^2)^{1/2}$, where $I_0$ is the maximum signal intensity above background, $\sigma_{bg}^2$ is the variance of the background intensity values, and $\sigma_{I_0}^2$ is the true variance of the maximum signal intensity above the background. Since $w$ width is approximately equal to the wide-field diffraction limit (which for visible light is about 250 nm), the uncertainty of the fitted coordinate ($\Delta\sigma$) is approximately given by $\Delta\sigma \approx 250/\mathrm{SNR}$ (nm), which is ±10−15 nm in our case (three independent experiments, $n$ = 873). In addition, QDot blinking was used to ensure single-molecule events. For trajectory generation, raw data files were extracted to generate stacks of individual 16-bit TIF images and then processed with Matlab (the MathWorks, Inc., Natick, MA) routines originally developed by Jaqaman and colleagues.[36]

**Instantaneous Velocity.** The distribution of single step displacement over a time increment (100 ms in our case) was carried out to calculate the instantaneous velocity. For temporary lateral confinement of a diffusing protein due to local environmental constraints such as interaction with lipid rafts or cytoskeletal corrals, the motion pattern can be best described as anomalous subdiffusion.[37] The statistical distribution of instantaneous velocities is thus close to a Lévy function instead of a Gaussian function, which is given by $f(x) = [\pi r(1 + (x - x_0)/r)^2]^{-1}$, where $x_0$ is the location parameter (the best fit instantaneous movement) and $r$ represents the interquartile range (the half-width at half-maximum) of the fitted step distance, meaning the statistical dispersion of the probability distribution. For practical applications, the Lévy probability distribution function can be simplified as a truncated Cauchy distribution: $f(x) = [b(1 + (x - x_0)/a)^2]^{-1}$, where $a$ and $b$ are only treated as fit coefficients in the defined function, and the goodness of the fit is judged by the $R^2$ value. In all of our analyses, the $R^2$ values of the fit of instantaneous velocity are higher than 95%, indicating high reliability of our fits.

**Diffusion Coefficients and Membrane Confinement.** After exporting trajectory coordinates, mean-square displacement (MSD) values for individual trajectories were calculated according to the following formula:[24]

$$\mathrm{MSD}(n\Delta t) = \frac{1}{N-1-n}\sum_{j=1}^{N-1-n}\left[(x_r)^2 + (y_r)^2\right]$$

where [$x_r = x(j\Delta t + n\Delta t) - x(j\Delta t)$, $y_r = y(j\Delta t + n\Delta t) - y(j\Delta t)$, $x(t)$ and $y(t)$ are the coordinates of QDot at time $t$, $\Delta t$ is the time resolution, $N$ is total number of frames, and $n\Delta t$ is the time interval over which the MSD is calculated. To achieve statistical significance, single QDot trajectories without a minimum of 100 time steps were discarded.


dx.doi.org/10.1021/cn3000845 | ACS Chem. Neurosci. 2012, 3, 737−743

In a two-dimensional Brownian motion, also known as random walks, the MSD over time is linear. The standard method to calculate the diffusion coefficient $D$ is to perform a linear fit of MSD over time since the MSD is given by $\mathrm{MSD}(t) = 4D\Delta t$, where $\Delta t$ is the time resolution.

For the case of confined diffusion, which is evident by a negative curvature on the MSD over time plot, we followed the method described by Daumas et al.[24] The MSD is given by

$$\mathrm{MSD}(t) = 2L^2(1 - e^{-t/\tau}) + 4D_M\tau \quad \text{and} \quad \tau = \frac{L^2}{2D_\mu}$$

where a short-term diffusion coefficient, $D_\mu$, is used to describe a rapid, "microscopic" diffusion behavior, and a long-term diffusion coefficient, $D_M$, indicates a slower, "macroscopic" movement. $L$ is the characteristic size of the short-term confining domain, and $\tau$ is the so-called "equilibration" or "relaxation" time on the short time scales.

## ■ ASSOCIATED CONTENT

### Supporting Information

Schematic of the optical setup of the microscope and the nondirectional random walk of membrane diffusion of AMP QDots. This material is available free of charge via the Internet at http://pubs.acs.org.

## ■ AUTHOR INFORMATION


### Corresponding Author

*E-mail address: sandra.j.rosenthal@vanderbilt.edu.



### Funding

This work was supported by a grant from the National Institute of Health (RO1EB003728). J.C.C. acknowledges the research fellowship from the Vanderbilt Institute of Nanoscale Science and Engineering (VINSE)


### Notes

The authors declare no competing financial interest.

## ■ ACKNOWLEDGMENTS


The authors thank Drs. David Piston, Alessandro Ustione, and Sam Wells and the VU Cell Imaging Shared Resource for help with the single-molecule microscopy.


## ■ REFERENCES


(1) Munro, S. (2003) Lipid rafts: Elusive or illusive? *Cell 115*, 377–388.

(2) Allen, J. A., Halverson-Tamboli, R. A., and Rasenick, M. M. (2007) Lipid raft microdomains and neurotransmitter signalling. *Nat. Rev. Neurosci. 8*, 128–140.

(3) Lingwood, D., and Simons, K. (2010) Lipid rafts as a membrane-organizing principle. *Science 327*, 46–50.

(4) Korade, Z., and Kenworthy, A. K. (2008) Lipid rafts, cholesterol, and the brain. *Neuropharmacology 55*, 1265–1273.

(5) Lai, E. C. (2003) Lipid rafts make for slippery platforms. *J. Cell Biol. 162*, 365–370.

(6) Vrljic, M., Nishimura, S. Y., Moerner, W. E. (2004) Strengths and weaknesses of single-molecule tracking. Biophysical society discussions speaker paper 13, SP13 A-J.

(7) Joo, C., Balci, H., Ishitsuka, Y., Buranachai, C., and Ha, T. (2008) Advances in single-molecule fluorescence methods for molecular biology. *Annu. Rev. Biochem. 77*, 51–76.

(8) Sako, Y., and Yanagida, T. (2003) Single-molecule visualization in cell biology. *Nat. Rev. Mol. Cell Biol.*, SS1–SS5.

(9) Rosenthal, S. J., Chang, J. C., Kovtun, O., McBride, J. R., and Tomlinson, I. D. (2011) Biocompatible quantum dots for biological applications. *Chem. Biol. 18*, 10–24.

(10) Chang, J. C., Kovtun, O., Blakely, R. D., and Rosenthal, S. J. (2012) Labeling of neuronal receptors and transporters with quantum dots. *Wiley Interdiscip. Rev.: Nanomed. Nanobiotechnol.*, DOI: 10.1002/wnan.1186.

(11) Dahan, M., Levi, S., Luccardini, C., Rostaing, P., Riveau, B., and Triller, A. (2003) Diffusion dynamics of glycine receptors revealed by single-quantum dot tracking. *Science 302*, 442–445.

(12) Cui, B., Wu, C., Chen, L., Ramirez, A., Bearer, E. L., Li, W.-P., Mobley, W. C., and Chu, S. (2007) One at a time, live tracking of NGF axonal transport using quantum dots. *Proc. Natl. Acad. Sci. U.S.A. 104*, 13666–13671.

(13) Bouzigues, C., Morel, M., Triller, A., and Dahan, M. (2007) Asymmetric redistribution of GABA receptors during GABA gradient sensing by nerve growth cones analyzed by single quantum dot imaging. *Proc. Natl. Acad. Sci. U.S.A. 104*, 11251–11256.

(14) Chang, J. C., Tomlinson, I. D., Warnement, M. R., Ustione, A., Carneiro, A. M. D., Piston, D. W., Blakely, R. D., and Rosenthal, S. J. (2012) Single molecule analysis of serotonin transporter regulation using antagonist-conjugated quantum dots reveals restricted, p38 MAPK-dependent mobilization underlying uptake activation. *J. Neurosci. 32*, 8919–8929.

(15) Ralf, W., Bernhard, Z., and Michael, K. (2006) High-speed confocal fluorescence imaging with a novel line scanning microscope. *J. Biomed. Opt. 11*, No. 064011.

(16) Nirmal, M., Dabbousi, B. O., Bawendi, M. G., Macklin, J. J., Trautman, J. K., Harris, T. D., and Brus, L. E. (1996) Fluorescence intermittency in single cadmium selenide nanocrystals. *Nature 383*, 802–804.

(17) Yao, J., Larson, D. R., Vishwasrao, H. D., Zipfel, W. R., and Webb, W. W. (2005) Blinking and nonradiant dark fraction of water-soluble quantum dots in aqueous solution. *Proc. Natl. Acad. Sci. U.S.A. 102*, 14284–14289.

(18) Schmidt, T., Schutz, G. J., Baumgartner, W., Gruber, H. J., and Schindler, H. (1996) Imaging of single molecule diffusion. *Proc. Natl. Acad. Sci. U.S.A. 93*, 2926–2929.

(19) Cheezum, M. K., Walker, W. F., and Guilford, W. H. (2001) Quantitative comparison of algorithms for tracking single fluorescent particles. *Biophys. J. 81*, 2378–2388.

(20) Bentzen, E. L., Tomlinson, I. D., Mason, J., Gresch, P., Warnement, M. R., Wright, D., Sanders-Bush, E., Blakely, R., and Rosenthal, S. J. (2005) Surface modification to reduce nonspecific binding of quantum dots in live cell assays. *Bioconjugate Chem. 16*, 1488–1494.

(21) Warnement, M. R., Tomlinson, I. D., Chang, J. C., Schreuder, M. A., Luckabaugh, C. M., and Rosenthal, S. J. (2008) Controlling the reactivity of ampiphilic quantum dots in biological assays through hydrophobic assembly of custom PEG derivatives. *Bioconjugate Chem. 19*, 1404–1413.

(22) Orlandi, P. A., and Fishman, P. H. (1998) Filipin-dependent inhibition of cholera toxin: evidence for toxin internalization and activation through caveolae-like domains. *J. Cell Biol. 141*, 905–915.

(23) Kenworthy, A. K., Petranova, N., and Edidin, M. (2000) High-resolution FRET microscopy of cholera toxin B-subunit and GPI-anchored proteins in cell plasma membranes. *Mol. Biol. Cell 11*, 1645–1655.

(24) Daumas, F., Destainville, N., Millot, C., Lopez, A., Dean, D., and Salome, L. (2003) Confined diffusion without fences of a G-protein-coupled receptor as revealed by single particle tracking. *Biophys. J. 84*, 356–366.

(25) Saxton, M. J., and Jacobson, K. (1997) Single-particle tracking: Applications to membrane dynamics. *Annu. Rev. Biophys. Biomol. Struct. 26*, 373–399.

(26) Murcia, M. J., Minner, D. E., Mustata, G.-M., Ritchie, K., and Naumann, C. A. (2008) Design of quantum dot-conjugated lipids for long-term, high-speed tracking experiments on cell surfaces. *J. Am. Chem. Soc. 130*, 15054–15062.

(27) Schutz, G. J., Kada, G., Pastushenko, V. P., and Schindler, H. (2000) Properties of lipid microdomains in a muscle cell membrane visualized by single molecule microscopy. *EMBO J. 19*, 892−901.
(28) Eggeling, C., Ringemann, C., Medda, R., Schwarzmann, G., Sandhoff, K., Polyakova, S., Belov, V. N., Hein, B., von Middendorff, C., Schonle, A., and Hell, S. W. (2009) Direct observation of the nanoscale dynamics of membrane lipids in a living cell. *Nature 457*, 1159−1162.
(29) Andrews, N. L., Lidke, K. A., Pfeiffer, J. R., Burns, A. R., Wilson, B. S., Oliver, J. M., and Lidke, D. S. (2008) Actin restricts FcepsilonRI diffusion and facilitates antigen-induced receptor immobilization. *Nat. Cell Biol. 10*, 955−963.
(30) Fabien, P., Xavier, M., Gopal, I., Emmanuel, M., Hsiao-Ping, M., and Shimon, W. (2009) Dynamic partitioning of a glycosyl-phosphatidylinositol-anchored protein in glycosphingolipid-rich microdomains imaged by single-quantum dot tracking. *Traffic 10*, 691−712.
(31) Burli, T., Baer, K., Ewers, H., Sidler, C., Fuhrer, C., and Fritschy, J. M. (2010) Single particle tracking of alpha7 nicotinic AChR in hippocampal neurons reveals regulated confinement at glutamatergic and GABAergic perisynaptic sites. *PLoS One 5*, No. e11507.
(32) Groc, L., Lafourcade, M., Heine, M., Renner, M., Racine, V., Sibarita, J. B., Lounis, B., Choquet, D., and Cognet, L. (2007) Surface trafficking of neurotransmitter receptor: comparison between single-molecule/quantum dot strategies. *J. Neurosci. 27*, 12433−12437.
(33) Wieser, S., and Schutz, G. J. (2008) Tracking single molecules in the live cell plasma membrane-Do's and Don't's. *Methods 46*, 131−140.
(34) Lidke, D. S., Nagy, P., Heintzmann, R., Arndt-Jovin, D. J., Post, J. N., Grecco, H. E., Jares-Erijman, E. A., and Jovin, T. M. (2004) Quantum dot ligands provide new insights into erbB/HER receptor-mediated signal transduction. *Nat. Biotechnol. 22*, 198−203.
(35) White, L. A., Eaton, M. J., Castro, M. C., Klose, K. J., Globus, M. Y., Shaw, G., and Whittemore, S. R. (1994) Distinct regulatory pathways control neurofilament expression and neurotransmitter synthesis in immortalized serotonergic neurons. *J. Neurosci. 14*, 6744−6753.
(36) Jaqaman, K., Loerke, D., Mettlen, M., Kuwata, H., Grinstein, S., Schmid, S. L., and Danuser, G. (2008) Robust single-particle tracking in live-cell time-lapse sequences. *Nat. Methods 5*, 695−702.
(37) Martin, D. S., Forstner, M. B., and Kas, J. A. (2002) Apparent subdiffusion inherent to single particle tracking. *Biophys. J. 83*, 2109−2117.